

Comparison of mixed-Higgs scenarios in the NMSSM and the MSSM

Radovan Dermíšek¹ and John F. Gunion²

¹*School of Natural Sciences, Institute for Advanced Study, Princeton, New Jersey 08540, USA*

²*Department of Physics, University of California at Davis, Davis, California 95616, USA*

(Received 17 September 2007; published 22 January 2008)

We study scenarios in the minimal and next-to-minimal supersymmetric models in which the lightest CP -even Higgs boson can have mass below the 114 GeV standard model LEP limit by virtue of reduced ZZ coupling due to substantial mixing among the Higgs bosons. We pay particular attention to the size of corrections from superpartners needed for these scenarios to be viable and point to boundary conditions at large scales which lead to these scenarios while at the same time keeping electroweak fine-tuning modest in size. We find that naturalness of electroweak symmetry breaking in the mixed-Higgs scenarios of both models points to the same region of soft supersymmetry breaking terms as in the decoupled scenarios with mass of the CP even Higgs boson above 114 GeV, namely those leading to large mixing in the stop sector at the electroweak scale, especially if we also require that the lightest CP -even Higgs explains the Higgs-like LEP events at ~ 98 GeV.

DOI: [10.1103/PhysRevD.77.015013](https://doi.org/10.1103/PhysRevD.77.015013)

PACS numbers: 14.80.Cp, 12.60.Jv

I. INTRODUCTION

Supersymmetry cures the naturalness/hierarchy problem associated with the quadratically divergent 1-loop corrections to the Higgs boson mass via the introduction of superpartners for each SM particle. So long as the superpartners have mass somewhat below 1 TeV, the cancellation is not particularly extreme and the hierarchy/naturalness problem associated with the quadratic divergences is ameliorated. However, there remains the question of how finely the GUT-scale parameters must be adjusted in order to get appropriate electroweak symmetry breaking, that is to say correctly predict the observed value of m_Z . LEP limits on a SM-like Higgs boson play a crucial role here.

Supersymmetric models most naturally predict that the lightest Higgs boson, generically h , has couplings to ZZ and $f\bar{f}$ pairs of SM strength (such an h is termed 'SM-like') and that it has a mass closely correlated to m_Z , typically lying in the range $\lesssim 105$ GeV for stop masses $\lesssim 500$ GeV, with an upper bound, for example, of $\lesssim 135$ GeV in the MSSM for stop masses ~ 1 TeV and large stop mixing. If the stop masses are large, the predicted value of m_Z is very sensitive to the GUT-scale parameters. Such sensitivity is termed "fine-tuning." Models with minimal fine-tuning provide a much more natural explanation of the Z mass than those with a high level of fine-tuning. The degree of fine-tuning required is thus quite closely related to the constraints on a SM-like h , and these in turn depend on how it decays.

The SM and the MSSM predict that $h \rightarrow b\bar{b}$ decays are dominant and LEP has placed strong constraints on $e^+e^- \rightarrow Zh \rightarrow Zb\bar{b}$. The limits on the effective coupling

$$C_{\text{eff}}^{2b} \equiv \left[\frac{g_{ZZh}^2}{g_{ZZh_{\text{SM}}}^2} \right] B(h \rightarrow b\bar{b}) \quad (1)$$

are such that $m_h < 114$ GeV is excluded for a SM-like h

that decays primarily to $b\bar{b}$. For $m_{\text{SUSY}} \lesssim 1$ TeV, most of CP -conserving MSSM parameter space is ruled out by this LEP limit. There are three surviving parts of MSSM parameter space. The first such part is characterized by at least one large stop mass at or above a TeV at scale m_Z . In this case, it is always the case that to predict the observed m_Z requires very careful adjustment, i.e. fine-tuning, of the GUT-scale parameters (either the Higgs mass-squared or μ^2) with accuracies better than 1% (the smaller the percentage accuracy required, the more fine-tuned is the model). The second part of MSSM parameter space that is consistent with LEP limits by virtue of having $m_h > 114$ GeV is that where mixing in the stop sector is large (i.e. $|A_t|/\bar{m}_t$ is large), and where $\bar{m}_t \equiv [\frac{1}{2}(m_{t_1}^2 + m_{t_2}^2)]^{1/2} \gtrsim 300$ GeV and $A_t \lesssim -500$ GeV (all at scale m_Z). This was explored in our previous paper, where we found that fine-tuning could be improved to about the 3% level. The third part of MSSM parameter space consistent with LEP limits is that where strong mixing between the two CP -even scalars of the model takes place, as arises when the CP -odd A has mass $m_A \sim 100$ GeV. In this region, the lightest CP -even Higgs has mass somewhat below the SM LEP limit of 114 GeV, as allowed by virtue of reduced ZZ coupling due to the mixing, and the heavier CP -even Higgs boson has mass slightly above this value. A mass $m_H > 114$ GeV is achieved by virtue of both the effects of Higgs mixing and large radiative corrections from the stop sector. However, because of the Higgs mixing the latter stop sector corrections need not be as large as in the parts of parameter space for which $m_h > 114$ GeV. In the first part of this paper, we explore this third sector of MSSM parameter space in detail. It is characterized by the extension of the first two regions to smaller stop masses or to smaller $|A_t|/\bar{m}_t$. The first region is extended to stop masses of $\bar{m}_t \gtrsim 600$ GeV, leading to fine-tuning of order 2%. The

second region is extended to somewhat smaller \bar{m}_t and significantly smaller ratio of $|A_t|/\bar{m}_t$, for which we find that the GUT-scale parameters must be chosen with an accuracy of at least 6.5%. This is a significant decrease of fine-tuning relative to the other cases.

In the second part of the paper, we consider mixed-Higgs scenarios in the next-to-minimal supersymmetric model (NMSSM) yielding a lightest Higgs boson h_1 with $m_{h_1} < 114$ GeV that escapes LEP limits by virtue of Higgs mixing yielding reduced ZZh_1 coupling. Two basic types of Higgs mixing can yield reduced ZZh_1 coupling while keeping fine-tuning to a not too unacceptable level: (i) mixing of the two doublet Higgs fields analogous to MSSM mixed-Higgs scenarios; and (ii) mixing of the doublet Higgs fields with the singlet Higgs field. In NMSSM case (i), our scans have found parameters yielding MSSM-like mixed-Higgs scenarios with the same level of fine-tuning as in mixed-Higgs MSSM scenarios, i.e. $\sim 6.5\%$. In NMSSM case (ii), we find it is also possible to reduce the GUT-scale parameter tuning required for correct EWSB to the level of $\sim 6.5\%$. We will present details of Higgs masses and GUT-scale parameters associated with these scenarios.

Although not the focus of this paper, the NMSSM mixed-Higgs scenarios should always be thought of in comparison to the very natural $\sim 17\%$ fine-tuning scenarios where the h_1 is very SM-like and has mass $m_{h_1} \sim 100$ GeV. In this case, see [1–3], the h_1 evades LEP limits by virtue of its primary decay being $h_1 \rightarrow a_1 a_1$ where $m_{a_1} < 2m_b$ so that the rate for $e^+ e^- \rightarrow Zh_1 \rightarrow Z + b's$ (where $b's$ refers to any final state with 2 or more $b's$) is small.¹ The attractiveness of this scenario is not only that it is not at all fine-tuned, but also: i) a SM-like Higgs with mass near 100 GeV is strongly preferred by precision electroweak measurements; and ii) these scenarios with large $B(h_1 \rightarrow a_1 a_1)$ typically predict [2] an excess in the $e^+ e^- \rightarrow Z + b's$ quite consistent with well-known 2.3σ excess in the LEP data for $M_{b's} \sim 98$ GeV [8]. Meanwhile, there are no current limits on the $Zh_1 \rightarrow Za_1 a_1 \rightarrow Z\tau^+ \tau^- \tau^+ \tau^-$ final state for $m_{h_1} \gtrsim 87$ GeV [9]. And limits in the case of $a_1 \rightarrow$ jets run out at still lower m_{h_1} .

In order to quantify fine-tuning, we employ the measure

$$F \equiv \text{Max}_p F_p \equiv \text{Max}_p \left| \frac{d \log m_Z}{d \log p} \right|, \quad (2)$$

where the parameters p comprise all GUT-scale soft-SUSY-breaking parameters. Above, we used F^{-1} in percent to express the degree of fine-tuning. The larger the fine-tuning F , the more finely the most sensitive GUT-scale parameter must be tuned (adjusted) as a percentage of its nominal value.

¹The importance of Higgs to Higgs decays was first made apparent in [4,5]. Further experimental implications of such decays were explored in Refs. [6,7].

While there are many earlier papers that have considered mixed-Higgs scenarios in the context of both the MSSM [10–16] and NMSSM (or other singlet extensions of the MSSM) [17–20], most did not consider the fine-tuning issue. Only a few papers [15–17] have studied the correlations between fine-tuning and Higgs mixing. This paper will extend these latter studies, fully exploring all of parameter space.

II. MSSM

In the MSSM, the CP -even Higgs mass-squared matrix in the basis (H_d, H_u) is given as:

$$M \simeq \begin{pmatrix} m_A^2 s_\beta^2 + m_Z^2 c_\beta^2 & -(m_A^2 + m_Z^2) s_\beta c_\beta \\ -(m_A^2 + m_Z^2) s_\beta c_\beta & m_Z^2 s_\beta^2 + m_A^2 c_\beta^2 + \Delta \end{pmatrix}, \quad (3)$$

where m_A is the mass of the CP odd Higgs boson, m_Z is the mass of the Z boson, $\tan \beta = v_u/v_d$ is the ratio of the vacuum expectation values of the two Higgs doublets and we use the shorthand notation $c_\beta = \cos \beta$ and $s_\beta = \sin \beta$. Finally, Δ is the SUSY correction to the 2-2 element of M which is dominated by the contributions from stop loops and thus depends on stop masses and the mixing in the stop sector. It is the size of this correction which is relevant for the discussion of fine-tuning of electroweak symmetry breaking.

The mass eigenstates are defined as follows:

$$\begin{pmatrix} H \\ h \end{pmatrix} = \begin{pmatrix} c_\alpha & s_\alpha \\ -s_\alpha & c_\alpha \end{pmatrix} \begin{pmatrix} H_d \\ H_u \end{pmatrix}, \quad (4)$$

and the coupling squared of the lighter CP -even Higgs boson to ZZ divided by the standard model value is given as:

$$\xi^2 = \frac{g_{ZZh}^2}{g_{ZZh_{\text{SM}}}^2} = \sin^2(\beta - \alpha). \quad (5)$$

(Note that in the notation of the NMSSM section of this paper, an equivalent notation would be $C_V^2(h)$ in place of ξ^2 .) Introducing a dimensionless quantity:

$$r_\Delta = \frac{\Delta}{m_Z^2} \quad (6)$$

and assuming $\tan \beta > \text{few}$ we can rewrite the CP -even Higgs mass-squared matrix as

$$M \simeq \begin{pmatrix} m_A^2 & -(m_Z^2 + m_A^2) s_\beta c_\beta \\ -(m_Z^2 + m_A^2) s_\beta c_\beta & m_Z^2(1 + r_\Delta) \end{pmatrix}. \quad (7)$$

Let us discuss the Higgs sector in two limits:

- (i) $m_A \gg m_Z$ —decoupled Higgs scenario: the lighter CP -even Higgs boson originates from H_u , $\alpha \simeq 0$, its mass is $m_h^2 \simeq m_Z^2(1 + r_\Delta)$ and it has SM-like ZZ coupling, $\xi^2 \simeq 1$.
- (ii) $m_A^2 < m_Z^2(1 + r_\Delta)$ —mixed-Higgs scenario: the lighter CP -even Higgs boson originates mainly from H_d , $m_h \simeq m_A$, and it has reduced ZZ coupling, $\xi^2 \ll 1$.

The heavier Higgs originates from H_u , its mass is $m_H^2 \simeq m_Z^2(1 + r_\Delta)$ and it has SM-like ZZ coupling. Without off-diagonal elements (mixing) in the Higgs mass-squared matrix, both scenarios require exactly the same size for the SUSY correction, Δ , and thus the same level of EWSB fine-tuning, in spite of the fact that in the mixed-Higgs scenario the lighter Higgs is well below the LEP limit of 114.4 GeV on the SM Higgs boson. The reason is that it is the SM-like Higgs (the Higgs with near maximal ZZ coupling) which has to be pushed above the LEP limit irrespectively of the fact that it is the heavier of the two.

The off-diagonal element in the Higgs mass-squared matrix makes the heavier eigenvalue heavier and the lighter eigenvalue lighter and thus, while in the usual decoupled scenario it decreases the mass of the SM-like Higgs boson, in the mixed-Higgs scenario it increases the mass of the SM-like Higgs boson. Thus, in the presence of mixing, the SUSY correction from the stop sector does not have to be as large in the mixed-Higgs scenario as in the decoupled scenario.² However, the mixing can be used to increase the Higgs boson mass only to some extent. First of all, the mixing term is proportional to $s_\beta c_\beta$ and so for small or large $\tan\beta$ it is negligible. For moderate $\tan\beta$, ZZ couples almost entirely to H_u , but the mixing term in M can still lead to the ZZ coupling being shared between the two Higgs mass eigenstates. However, the off-diagonal term cannot be too large without the light, mainly H_d , mass state having a ξ^2 that exceeds the very strong limits on this quantity for any Higgs with mass well below the LEP limit.

For given $\tan\beta$ and m_A we can determine the minimal value of the SUSY correction needed for both scenarios to be viable. In Fig. 1, we plot contours of constant m_h , m_H and ξ^2 in the m_A — r_Δ plane for $\tan\beta = 10$. We easily recognize the behavior of Higgs masses. In the decoupling limit, $m_A \gg m_Z$, the mass of the light CP -even Higgs boson does not depend on m_A and the mass of the heavy CP -even Higgs boson scales linearly with m_A . The masses of both Higgses increase with increased radiative correction to the 2-2 element of the Higgs mass-squared matrix. We see that the mixed-Higgs scenario is viable for $r_\Delta \gtrsim 0.5$ while the decoupled scenario requires $r_\Delta \gtrsim 0.65$. Thus, the mixed-Higgs scenario requires a somewhat smaller contribution from the stop sector. On the other hand, this scenario works only in a limited range of m_A since the soft-SUSY-breaking parameters $m_{H_d}^2$ and $m_{H_u}^2$ have to be carefully adjusted relative to one another given the relation

$$m_A^2 \simeq m_{H_d}^2 - m_{H_u}^2 - m_Z^2 \quad (8)$$

at tree level for $\tan\beta > \text{few}$. In the above equation, $m_{H_d}^2$ and $m_{H_u}^2$ are the weak-scale values. The particular values to

²This possibility of increasing the Higgs mass by mixing was suggested as a solution to the fine-tuning problem of EWSB in Ref. [15].

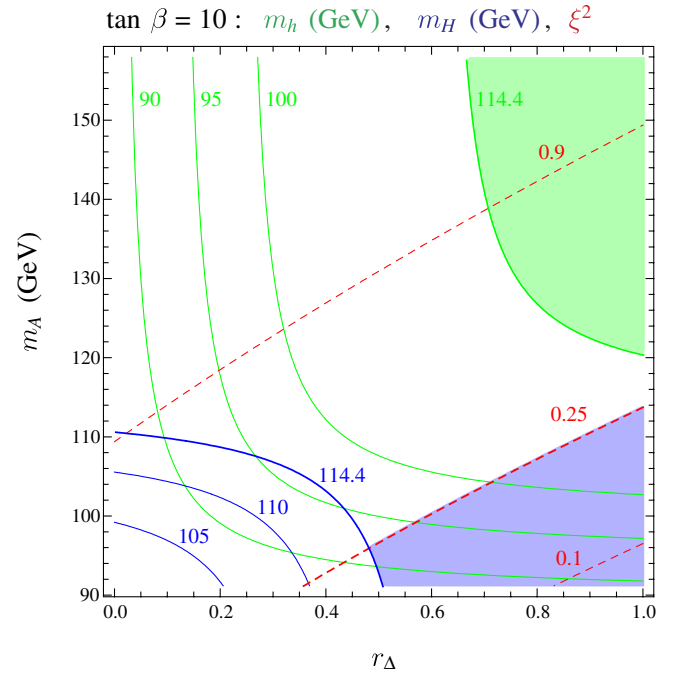


FIG. 1 (color online). Contours of constant m_h (green), m_H (blue), and ξ^2 (red) in the m_A — r_Δ plane for $\tan\beta = 10$. The green shaded region represents the allowed region for the decoupled scenario (the light CP -even Higgs is above the LEP limit on the mass of the SM Higgs boson) and the blue shaded region represents the allowed region for the mixed-Higgs scenario (the heavy CP -even Higgs is above the LEP limit on the mass of the SM Higgs boson and the coupling squared of the light Higgs to ZZ is below the LEP limit, $\xi^2 \lesssim 0.25$ for $m_h \sim 100$ GeV).

which they evolve at the GUT scale will depend on many of the other weak-scale parameters. Thus, in order to achieve the required relation of Eq. (8), all of the various GUT-scale parameters will have to be closely correlated in a very particular way. Furthermore, as we will see, the improvement in naturalness is limited to a very small window in $\tan\beta$, which implies also a small window for the B_μ parameter due to the relation

$$m_A^2 \simeq B_\mu \tan\beta. \quad (9)$$

For smaller $\tan\beta$, the contribution from mixing is more significant and so the heavy Higgs can be heavier than 114.4 GeV for a smaller value of the SUSY correction, Δ . However, the off-diagonal term in M is increased and Higgs mixing is larger, which significantly increases ξ^2 . In Fig. 2 (left) we see that the mixed-Higgs scenario is not viable for $\tan\beta = 5$. (Note that we do not show $m_A < 90$ GeV in the plots. This is because at fixed r_Δ both m_h and m_H decrease as m_A decreases and $Z \rightarrow h + A$ limits from LEP enter.) For $\tan\beta$ significantly above 10, the Higgs-mixing induced by the off-diagonal element of M is negligible and thus the mixed-Higgs scenario requires basically the same radiative correction as the decoupled one. This is clearly visible in the behavior of the masses of

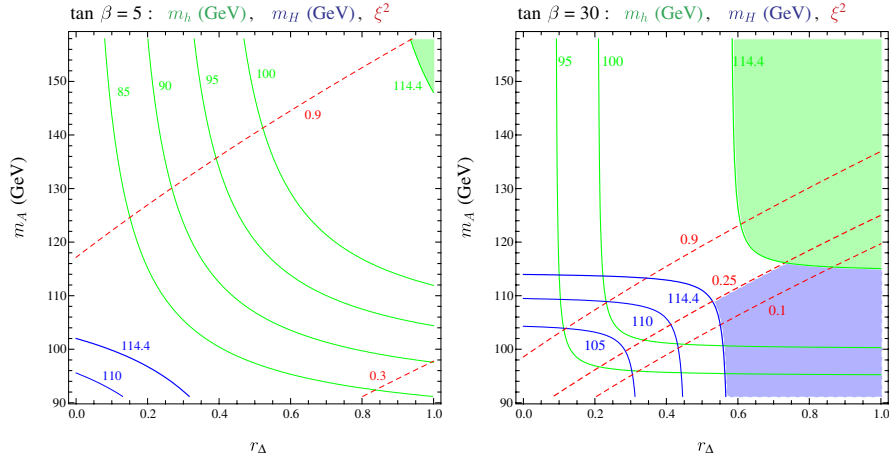


FIG. 2 (color online). Contours of constant m_h (green), m_H (blue), and ξ^2 (red) in m_A — r_Δ plane for $\tan\beta = 5$ (left) and $\tan\beta = 30$ (right). The meaning of the shaded regions is the same as in Fig. 1.

the light and heavy CP -even Higgses for $\tan\beta = 30$, see Fig. 2 (right).

It is worth noting that for $\tan\beta \sim 20$ the mixed-Higgs scenario can yield both the 98 GeV and the 116 GeV excesses of Higgs-like events observed at LEP. This is illustrated in Fig. 3. For $\tan\beta = 20$, we see that in the vicinity of $[m_A, r_\Delta] \sim [100 \text{ GeV}, 0.6]$ the mass of the light Higgs is about 98 GeV with $\xi^2 \sim 0.1$ (as needed to explain the excess of Higgs-like events at 98 GeV) while the heavy Higgs has a mass of about 116 GeV (and $g_{ZZH}^2/g_{ZZH_{SM}}^2 \sim 0.9$). This possibility was studied in detail in Ref. [13]. It is clear from Fig. 3 that this mixed-Higgs scenario that ex-

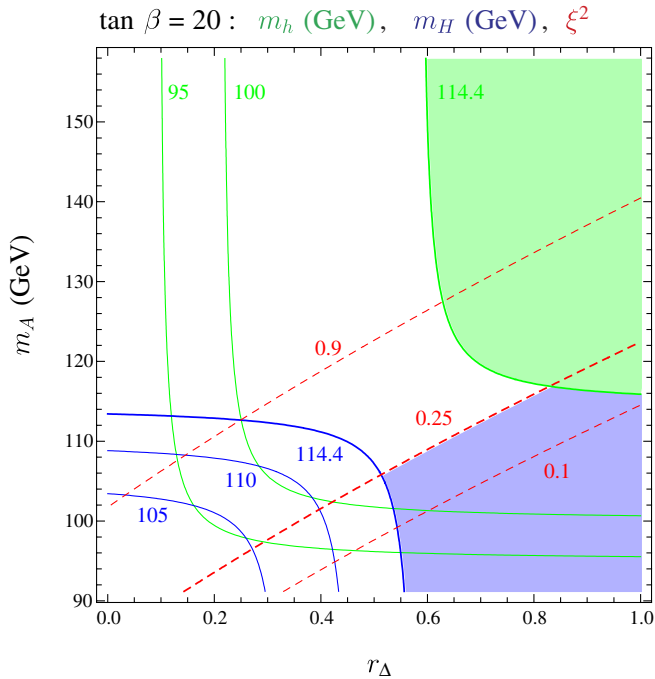


FIG. 3 (color online). Contours of constant m_h (green), m_H (blue), and ξ^2 (red) in m_A — r_Δ plane for $\tan\beta = 20$. The meaning of shaded regions is the same as in Fig. 1.

plains simultaneously both the 98 GeV and 116 GeV LEP excesses of Higgs-like events requires basically the same size of SUSY correction, Δ , as the decoupled scenario and thus it works in the same region of SUSY parameter space.

From this simplified exercise we thus learn that LEP consistency of the mixed-Higgs scenario still requires a significant correction from the stop sector although somewhat smaller than the decoupled scenario. Now we proceed with a precise numerical analysis of the associated fine-tuning which closely follows the analysis outlined in Ref. [3]. Compared to our previous work, we designed a special scan to pick up mixed-Higgs scenarios which would occur very rarely in a random scan due to the relatively narrow range of m_A , or, alternatively, of m_{H_d} , required. In these scans, we employ the fixed value of $\tan\beta = 10$ (which our discussion has shown should give the most improvement on fine-tuning relative to the decoupled scenario) and fixed gaugino soft masses of $M_{1,2,3} = 100, 200, 300 \text{ GeV}$. We scan over all other soft-SUSY-breaking parameters, including μ , B_μ and the third generation (stop) parameters m_Q , m_U , m_D , and A_t , all defined at scale m_Z . For each set of these m_Z -scale parameter choices, we determine the values of all the soft parameters at the GUT scale, $M_U \sim 2 \times 10^{16} \text{ GeV}$, by renormalization group evolution. We then vary each GUT-scale parameter, p , in turn, and evolve back to scale m_Z to determine how much m_Z has changed. From this we compute F of Eq. (2). The resulting values of F are presented in Figs. 4 and 5 as a function of m_h , $\bar{m}_{\tilde{t}}$ and A_t . A blue + is plotted whenever there is a soft-SUSY-breaking scenario with $m_h < 114 \text{ GeV}$ that is excluded by LEP due to the fact that ξ^2 is too large. Overlaid on the blue +’s we plot a green diamond whenever there is a choice of soft-SUSY-breaking parameters yielding $m_h < 114 \text{ GeV}$ but with sufficiently reduced ZZh coupling (due to the effects of Higgs mixing) so as to not be excluded by LEP. A red \times is plotted whenever there is a soft-SUSY-

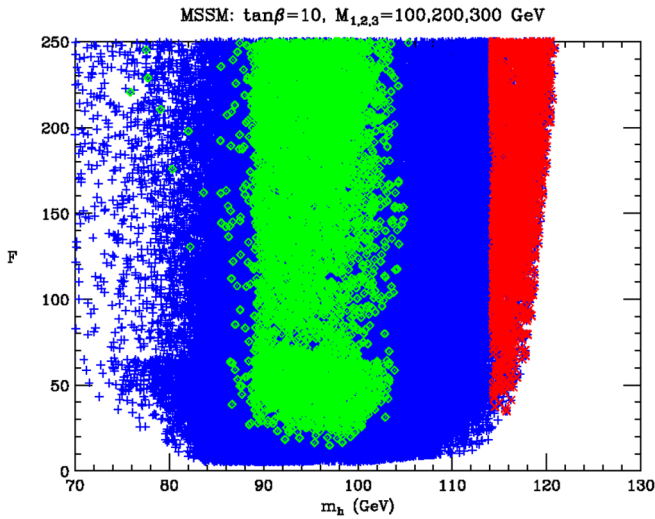


FIG. 4 (color online). Fine-tuning vs m_h for randomly generated MSSM parameter choices with $\tan\beta = 10$ and $M_{1,2,3}(m_Z) = 100, 200, 300$ GeV. Blue pluses correspond to parameter choices yielding $m_h < 114$ GeV that are ruled out by LEP limits on the Higgs mass and as a function of the ZZh coupling. Green diamonds are the mixed-Higgs scenarios with $m_h < 114$ GeV that satisfy LEP limits due to reduced ZZh coupling. Red crosses are points with $m_h > 114$ GeV—these automatically satisfy LEP limits.

breaking parameter set yielding $m_h > 114$ GeV—LEP constraints are automatically satisfied in this case.

In Fig. 4 we see that the mixed-Higgs scenarios (green diamonds) require m_A to be near ~ 90 – 100 GeV; fine-tuning can be as low as $F \sim 15.5$ (6.5% parameter tuning), a significant reduction compared to the decoupled scenario (red crosses) for which the minimal F is about 30. The least fine-tuned decoupled scenarios require large mixing in the stop sector, as shown in Fig. 5. From the same figure, we see that the mixed-Higgs scenarios extend the region of

SUSY parameter space allowed by the LEP constraints to slightly smaller stop masses and somewhat smaller mixing as compared to the decoupled (large m_A) scenarios with $m_h > 114$ GeV.

In conclusion, the level of fine-tuning in the mixed-Higgs scenario can be reduced to about 6.5% compared to the 3% fine-tuning needed in the decoupled Higgs scenario. However, this improvement happens only in a limited range of $\tan\beta$ (the results presented for $\tan\beta = 10$ are close to the optimal choice) and m_A . As a result, the mixed-Higgs scenario requires additional constraints on the m_{H_d} and B_μ parameters which are not constrained in the case of the decoupled Higgs scenario. For smaller $\tan\beta$ the mixed-Higgs scenario is not viable and for large $\tan\beta$ it requires the same level of fine-tuning as the decoupled Higgs solution.

The fact that the required magnitude of Δ is similar in the mixed and decoupled scenarios means that they both prefer the same region of SUSY parameter space, namely, that with large mixing in the stop sector. The mixed-Higgs scenario allows for continuation of this region to somewhat smaller mixing for optimal $\tan\beta$. The large mixing in the stop sector can be achieved either in models which generate a large top soft trilinear coupling, A_t , at a large scale or it can be achieved by renormalization group evolution in models which generate negative stop masses squared at a large scale [21].

III. MIXED AND UNMIXED HIGGS SCENARIOS IN THE NMSSM

The NMSSM is an extremely attractive model [4,22]. In particular, it provides a very elegant solution to the μ problem of the MSSM via the introduction of a singlet superfield \hat{S} . For the simplest possible scale invariant form of the superpotential, the scalar component of \hat{S} naturally

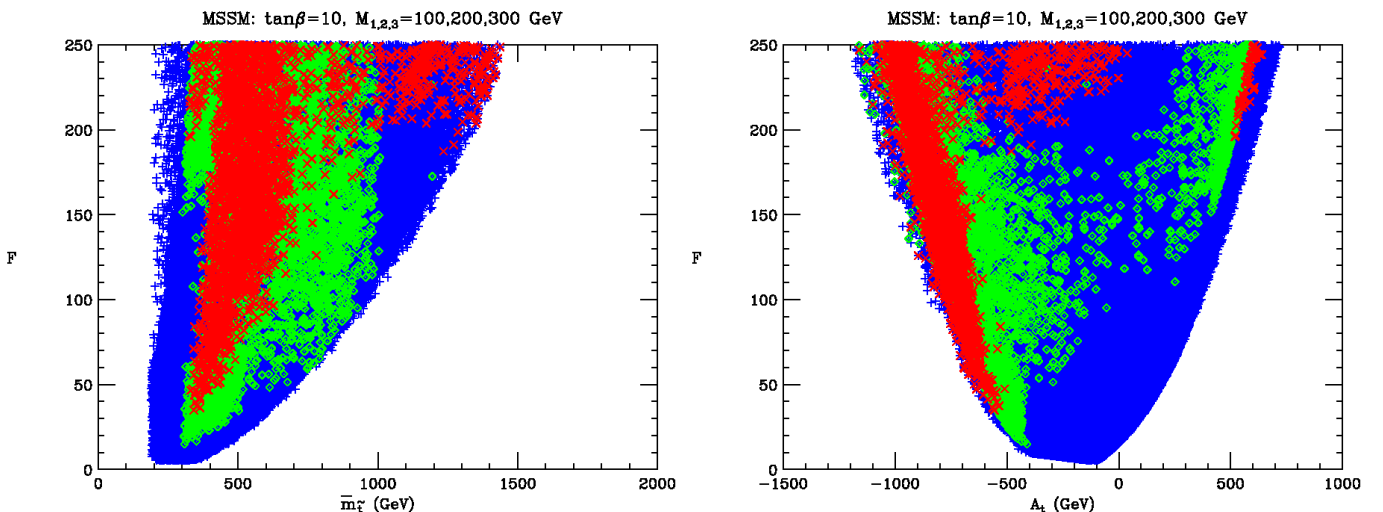


FIG. 5 (color online). Fine-tuning vs \bar{m}_t (left) and fine-tuning vs A_t (right) for randomly generated MSSM parameter choices with $\tan\beta = 10$ and $M_{1,2,3}(m_Z) = 100, 200, 300$ GeV. Point convention as in Fig. 4.

acquires a vacuum expectation value of the order of the SUSY breaking scale, giving rise to a value of μ of order the electroweak scale. The NMSSM is the simplest supersymmetric extension of the standard model in which the electroweak scale originates from the SUSY breaking scale only.

Apart from the usual quark and lepton Yukawa couplings, the scale invariant superpotential of the NMSSM is $W = \lambda \hat{S} \hat{H}_u \hat{H}_d + \frac{1}{3} \kappa \hat{S}^3$ depending on two dimensionless couplings λ , κ beyond the MSSM. [Hatted (unhatted) capital letters denote superfields (scalar superfield components).] The associated trilinear soft terms are $\lambda A_\lambda S H_u H_d + \frac{1}{3} \kappa A_\kappa S^3$. The final two input parameters are $\tan\beta = h_u/h_d$ and $\mu_{\text{eff}} = \lambda s$, where $h_u \equiv \langle H_u \rangle$, $h_d \equiv \langle H_d \rangle$, and $s \equiv \langle S \rangle$. The Higgs sector of the NMSSM is thus described by the six parameters λ , κ , A_λ , A_κ , $\tan\beta$, μ_{eff} . In addition, values must be input for the gaugino masses and for the soft terms related to the (third generation) squarks and sleptons that contribute to the radiative corrections in the Higgs sector and to the Higgs decay widths.

The particle content of the NMSSM differs from the MSSM by the addition of one CP -even and one CP -odd state in the neutral Higgs sector (assuming CP conservation), and one additional neutralino. The result is three CP -even Higgs bosons ($h_{1,2,3}$) two CP -odd Higgs bosons ($a_{1,2}$) and a total of five neutralinos $\tilde{\chi}_{1,2,3,4,5}^0$. While we denoted the CP -even and CP -odd neutral Higgs bosons of the MSSM as h , H and A , respectively, those of the NMSSM will be denoted by h_1 , h_2 , h_3 and a_1 , a_2 , respectively. In the latter case, our focus will be on the lightest states h_1 and a_1 . The NMHDECAY program [23], which includes most LEP constraints, allows easy exploration of Higgs phenomenology in the NMSSM.

The NMSSM study presented in this paper focuses on cases in which the lightest Higgs boson can have $m_{h_1} < 114$ GeV without violating LEP limits and without necessarily having the $h_1 \rightarrow a_1 a_1$, with $m_{a_1} < 2m_b$ decay being dominant. While it is true that this latter situation gives rise to models with the very least fine-tuning, there are alternative models with only modest fine-tuning in which $m_{h_1} < 114$ GeV but substantial Higgs mixing suppresses the ZZh_1 coupling sufficiently that the $e^+ e^- \rightarrow Z^* \rightarrow Zh_1$ production rate is reduced to an allowed level even if $h_1 \rightarrow b\bar{b}$ and/or $h_1 \rightarrow a_1 a_1 \rightarrow 4b$ decays are dominant.

This can occur in a number of ways. The first possibility is that the h_1 has substantial singlet S component. In such scenarios, it is typically the h_2 that is the most SM-like CP -even Higgs boson, but $m_{h_2} > 114$ GeV and LEP constraints do not apply to the h_2 . Another possibility is the analogue of the MSSM mixed-Higgs scenarios described in the preceding MSSM sections. For these, the h_1 and h_2 both have mass near 100 GeV and are primarily nonsinglet, but mix in such a way that the LEP limits are evaded. And, of course, there are LEP-allowed scenarios in which the h_1 mixes partly with the singlet and partly with the other

MSSM-like Higgs boson. We have performed a broad scan over NMSSM parameter space to look for and investigate the fine-tuning associated with scenarios of each type. As discussed below, not all the points of this type found in our scans are highly fine-tuned. There are specific parameter regions that produce points of each type that are only moderately fine-tuned for which the h_1 has $m_{h_1} < 114$ GeV but escapes LEP limits by virtue of small ZZh_1 coupling.

To be explicit, let us take $M_{1,2,3} = 100, 200, 300$ GeV and $\tan\beta = 10$, as before. We scan over a broad range of all other NMSSM parameters searching for points that: (a) are consistent with all constraints built into NMHDECAY; (b) obey the additional requirement that the effective $Z + b'$'s rate from Zh_1 production, as quantified via

$$\xi^2(Z + b's) \equiv \frac{g_{ZZh_1}^2}{g_{ZZh_{\text{SM}}}^2} [B(h_1 \rightarrow b\bar{b}) + B(h_1 \rightarrow a_1 a_1) \times [B(a_1 \rightarrow b\bar{b})]^2], \quad (10)$$

lies below the LEP limit on the $Z + 2b$ final state.³ Figure 6 shows the electroweak fine-tuning measure F as a function of m_{h_1} , m_{a_1} and m_{h_2} . In this, and all succeeding plots, we only show points with $F < 100$, corresponding to fine-tuning no worse than 1%. One sees (the blue + 's) the expected large number of points with low F , $m_{h_1} \sim 100$ GeV and $m_{a_1} < 2m_b$ that escape LEP limits by virtue of large $B(h_1 \rightarrow a_1 a_1 \rightarrow 4\tau)$.⁴ In addition, there are several classes of points with only somewhat higher minimum F that escape LEP limits. We detail these below. We note that the density of points in the various classes we shall discuss is somewhat a function of how we did the scanning. For instance, we worked hard to find MSSM-like mixed-Higgs scenarios, whereas we did not do so for the other mixed-Higgs scenarios. And some scan runs purposely deemphasized the (blue) + points that previous papers have focused on.

First, there are the (red) diamond-star points with an essentially pure singlet a_1 with $m_{a_1} \sim 50$ GeV and an h_1 with very SM-like ZZh_1 coupling and $m_{h_1} \sim 110$ GeV that escape LEP published limits by virtue of $h_1 \rightarrow a_1 a_1 \rightarrow 4\gamma$ being the dominant h_1 decay. As discussed in our previous paper, the fine-tuning of A_λ and A_κ needed to achieve an almost purely singlet a_1 is quite significant and, further, it is likely that a LEP analysis of the $Z + 4\gamma$ final state would eliminate these points. Nonetheless, we include them since

³This constraint can be stronger than necessary in cases where the $4b$ final state is dominant, for which it is known that LEP limits only imply $m_{h_1} \lesssim 110$ GeV. However, absent full LEP analysis on a point-by-point basis it is the safest approach available to us. Additional allowed points might emerge in a point-by-point approach.

⁴The very broad scans focused on mixed-Higgs scenarios performed for this paper did not pick up the very lowest F points that have $F \sim 6$ found in our specialized scans of earlier papers.

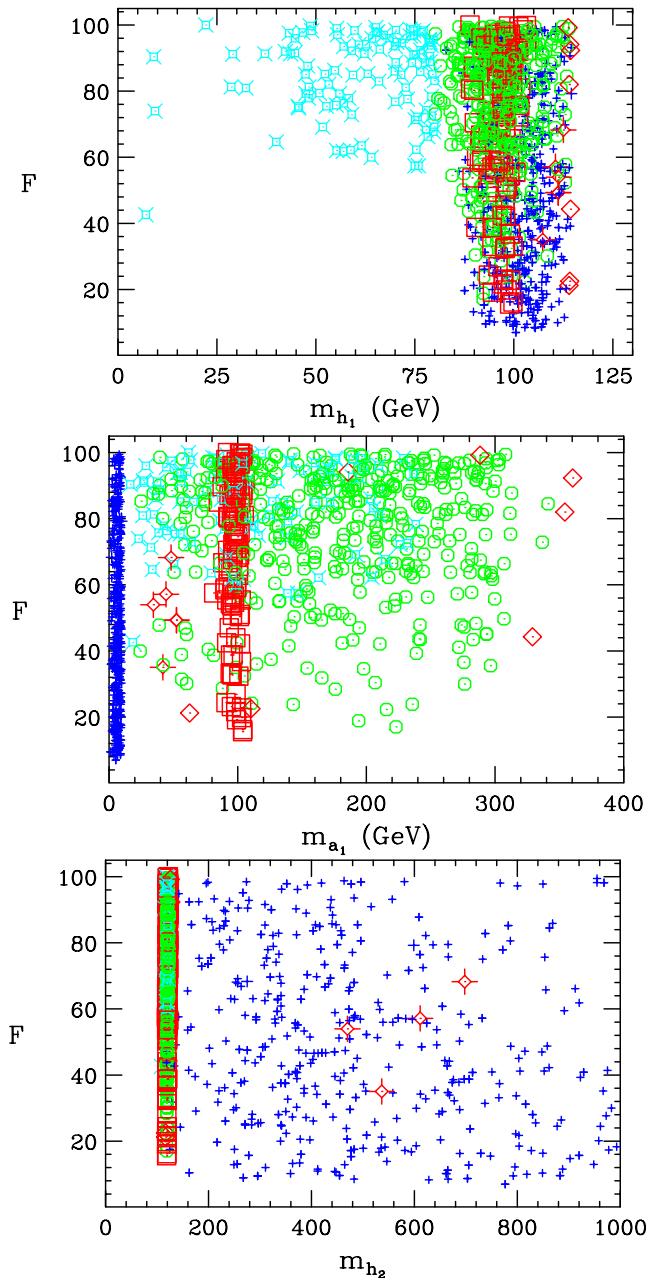


FIG. 6 (color online). For fixed $M_{1,2,3}(m_Z) = 100, 200, 300$ GeV and $\tan\beta = 10$ we plot: F vs m_{h_1} (top); F vs m_{a_1} (middle); and F vs m_{h_2} (bottom). In this and all succeeding plots, all points have $F < 100$ and $m_{h_1} < 114$ GeV. The blue + points are ones with a very SM-like ZZh_1 coupling that escape LEP limits because $m_{a_1} < 2m_b$ and $h_1 \rightarrow a_1 a_1 \rightarrow 4\tau$ or $4j$ decays are dominant. All other points have $m_{a_1} > 2m_b$. The definitions of the other points appear in the text.

they can have F as small as about 35, corresponding to about 3% parameter tuning to get proper EWSB.

The remaining points have $m_{a_1} > 2m_b$ (and $m_{h_1} < 114$ GeV) and escape LEP limits by virtue Higgs-mixing leading to suppressed ZZh_1 coupling. A discussion of the ZZh_1 coupling is appropriate before giving our classifica-

tion of these points. Defining

$$C_V^2(h_1) \equiv \frac{g_{ZZh_1}^2}{g_{ZZh_{SM}}^2}, \quad (11)$$

one has

$$C_V^2(h_1) = (\sin\beta S_{11} + \cos\beta S_{12})^2, \quad (12)$$

where the h_1 mixture is defined by

$$h_1 = S_{11}H_{uR} + S_{12}H_{dR} + S_{13}S_R, \quad (13)$$

and similarly for h_2 and h_3 . Here, the neutral Higgs fields are taken to be

$$H_u^0 = h_u + \frac{H_{uR} + iH_{uI}}{\sqrt{2}}, \quad H_d^0 = h_d + \frac{H_{dR} + iH_{dI}}{\sqrt{2}}$$

$$S = s + \frac{S_R + iS_I}{\sqrt{2}}, \quad (14)$$

with h_u, h_d, s being the vevs. We will similarly write

$$a_1 = P_{11}(\cos\beta H_{uI} + \sin\beta H_{dI}) + P_{12}S_I, \quad (15)$$

and similarly for a_2 . When $\tan\beta$ is large (as it is for this $\tan\beta = 10$ discussion), $\cos\beta$ is small and if S_{11} is small then $C_V^2(h_1) \ll 1$ is automatic.

In the figures, we have divided the remaining scenarios into four distinct categories.

- (1) The first large group of points (indicated by large cyan starred squares) are those for which $m_{h_1} < 80$ GeV (including very small m_{h_1}) and the h_1 is largely singlet, $|S_{13}| \sim 1$. The h_2 has $C_V^2(h_2) \sim 1$ but escapes LEP limits since $m_{h_2} > 114$ GeV; in fact, almost invariably $m_{h_2} \sim 120$ GeV for these points, with a few having m_{h_2} between 110 GeV and 118 GeV. The minimum F for this category of point is $F \sim 40$.
- (2) The second large group of points (indicated by large green, or darker, circles) have $m_{h_1} > 80$ GeV (clustered about $m_{h_1} \sim 100$ GeV) but have sufficiently suppressed $C_V^2(h_1)$ because the h_1 is predominantly singlet: $(S_{11}^2 + S_{12}^2) < 0.5$. These points have $|P_{11}| \sim 0$, implying that the a_1 is very nearly pure singlet. The h_2 has $m_{h_2} \sim 120$ GeV and $C_V^2(h_2) > 0.5$ for these points. The minimum F for these points is $F \sim 17$, or 6% fine-tuning, which, while not as good as the blue + points (which can reach down to $F \sim 6$ in a fuller scan), is not really too bad.
- (3) The third set of points are the large (red) plain diamonds. For these points, $0.5 \leq (S_{11}^2 + S_{12}^2) < 0.9$, $|S_{12}| < 0.1$, implying that the h_1 is mainly H_{uR} , and m_{h_1} is just below 114 GeV. Almost any value of $m_{a_1} \geq 60$ GeV (implying no $h_1 \rightarrow a_1 a_1$ decays) is possible and the a_1 is nearly purely singlet. The minimum F here is $F \sim 22$. These scenarios are remnants of the usual decoupled sce-

narios (for which $m_{h_1} > 114$ GeV and for which we found $F \sim 20$ in Ref. [3])—they instead have Higgs mass just slightly below 114 GeV and just enough Higgs mixing to escape LEP limits.

- (4) Points in the fourth and final set are those that are the NMSSM analogues of the MSSM points with strong mixing between the two doublet Higgs fields. These are indicated by the large (red) plain squares. These have $m_{a_1} \sim m_{h_1} \sim 100$ GeV, $(S_{11}^2 + S_{12}^2) > 0.9$ and $|P_{11}| \sim 1$, implying that both the a_1 and the h_1 have small singlet component. Typically, $|S_{12}| \sim 0.95$ and $|S_{11}| \sim 0.3$, implying that the h_1 is mainly H_{DR} . The minimum F for these MSSM-like mixed-Higgs scenarios found in our scans is $F \sim 16$. This is the same level as achieved for the mixed-Higgs scenarios in the MSSM scans discussed previously.

With regard to the 4th category above, it is useful to recall from Ref. [4] that the MSSM limit of the NMSSM is obtained in the limit of large s holding $\lambda s = \mu_{\text{eff}}$ fixed and κs fixed. Thus, we would expect that the red square points would tend to have small λ and κ . A later plot will show this tendency.

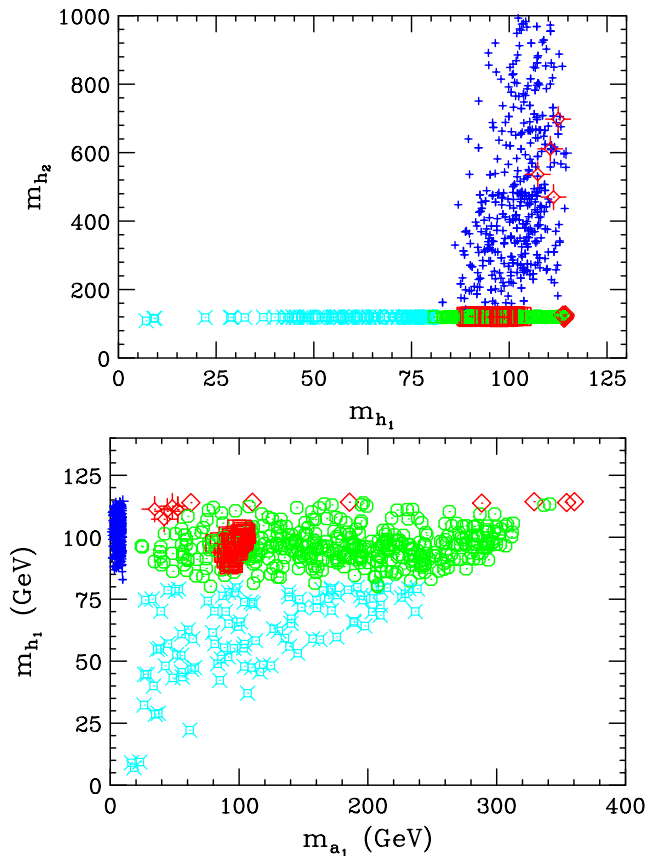


FIG. 7 (color online). For fixed $M_{1,2,3}(m_Z) = 100, 200, 300$ GeV and $\tan\beta = 10$ we plot: m_{h_2} vs m_{h_1} (top) and m_{h_1} vs m_{a_1} (bottom). Notation and conventions as in Fig. 6.

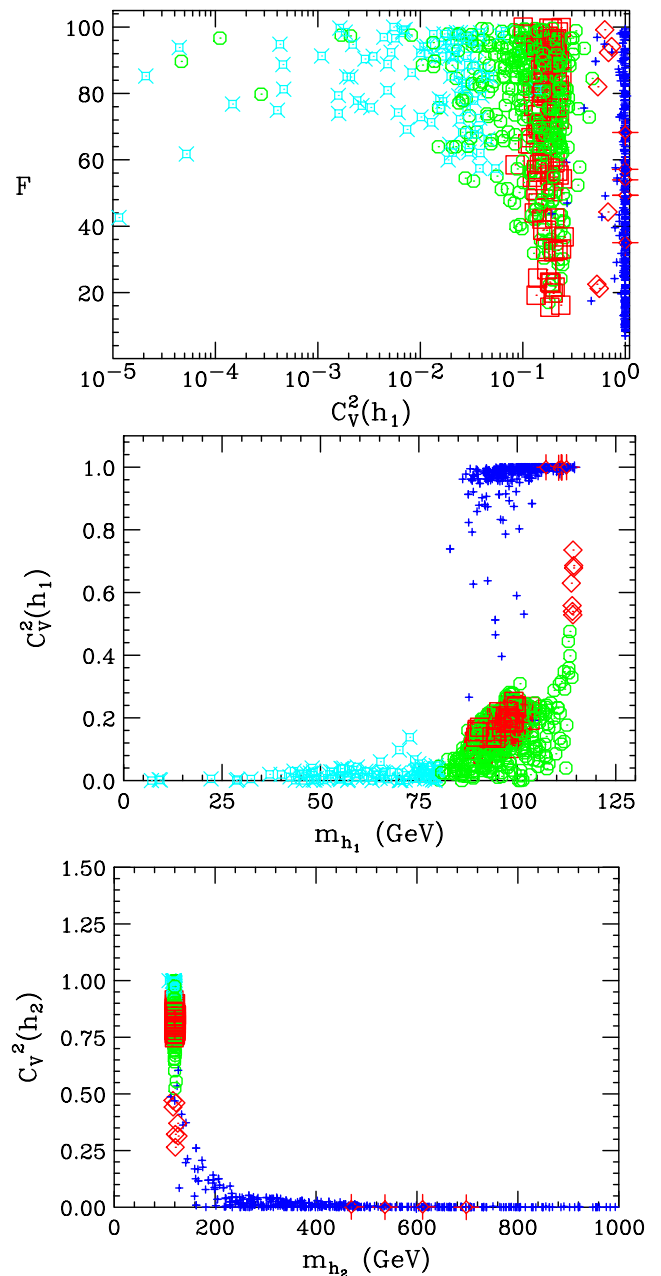


FIG. 8 (color online). For fixed $M_{1,2,3}(m_Z) = 100, 200, 300$ GeV and $\tan\beta = 10$ we plot F vs $C_V^2(h_1)$, $C_V^2(h_1)$ vs m_{h_1} and $C_V^2(h_2)$ vs m_{h_2} . Notation and conventions as in Fig. 6.

The various features of all categories of points are illustrated in detail in a series of figures. Correlations between m_{h_1} and m_{h_2} and between m_{h_1} and m_{a_1} for the points shown in Fig. 6 are shown in Fig. 7. Details regarding $C_V^2(h_1)$ and $C_V^2(h_2)$ are shown in Fig. 8. The above-described correlations involving the compositions of the h_1 and a_1 are made apparent in the plots of Figs. 9–11. Figure 12 shows m_{h_1} as a function of the S_{12} composition.

Figure 13 shows the LEP limit on $\xi^2(Z + b's)$ in comparison to the values for the points in our scan. The plain

(red) diamond and square points hug the LEP limit. The precipitous decline in the $\xi^2(Z + b's)$ limit as one passes below $m_{h_1} \sim 80$ GeV means that only points with $F \gtrsim 40-50$ are found in this region. As noted earlier, the limit imposed on ξ^2 is a bit too severe in cases where the h_1

branching ratio to $b\bar{b}$ is much smaller than that to $b\bar{b}b\bar{b}$ due to large $B(h_1 \rightarrow a_1 a_1)$ and $m_{a_1} > 2m_b$. However, this does not arise for either the diamond or square type points, all of which have $m_{h_1} < 2m_{a_1}$.

Correlations of these scenarios with various GUT-scale parameters are illuminating. In Fig. 14, we show F vs $m_{H_u}(M_U)$, $m_{H_d}(M_U)$ and $m_S(M_U)$, where negative m values

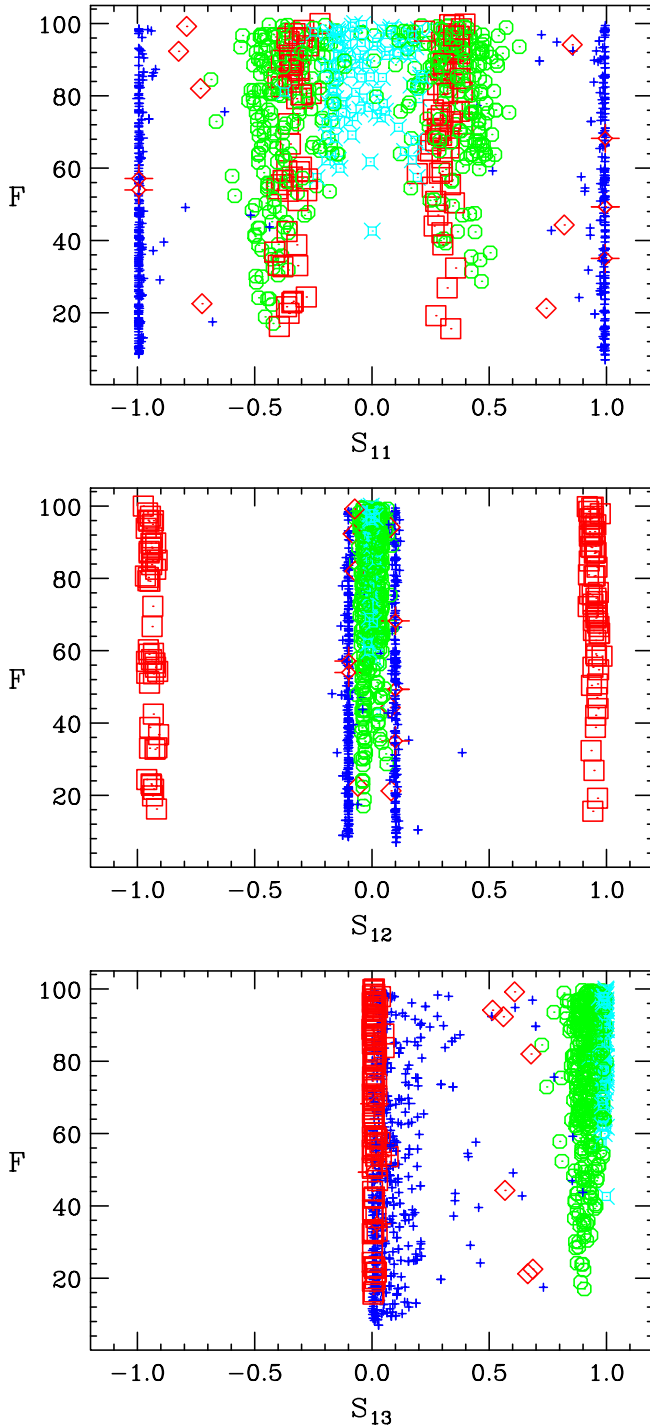


FIG. 9 (color online). For fixed $M_{1,2,3}(m_Z) = 100, 200, 300$ GeV and $\tan\beta = 10$ we plot: F vs S_{11} (top); F vs S_{12} (middle); and F vs S_{13} (bottom). Notation and conventions as in Fig. 6.

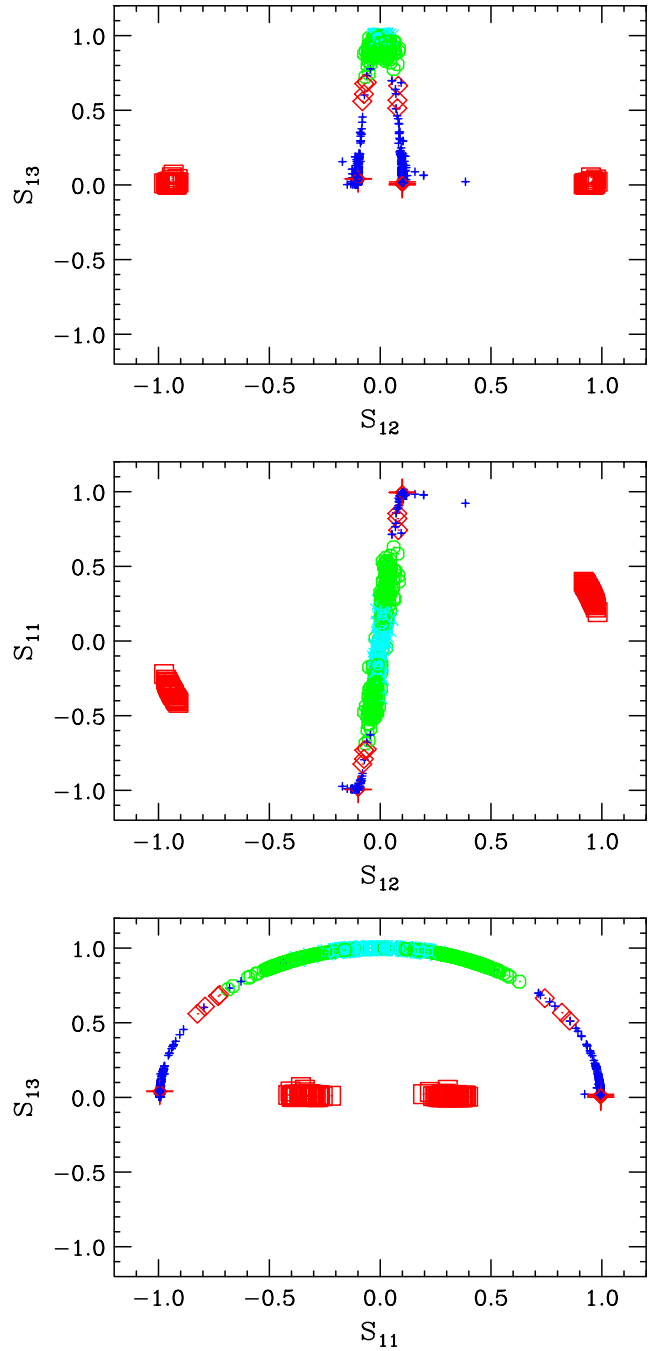


FIG. 10 (color online). For fixed $M_{1,2,3}(m_Z) = 100, 200, 300$ GeV and $\tan\beta = 10$ we plot: S_{13} vs S_{12} (top) and S_{11} vs S_{12} (middle) and S_{13} vs S_{11} (bottom). Notation and conventions as in Fig. 6.

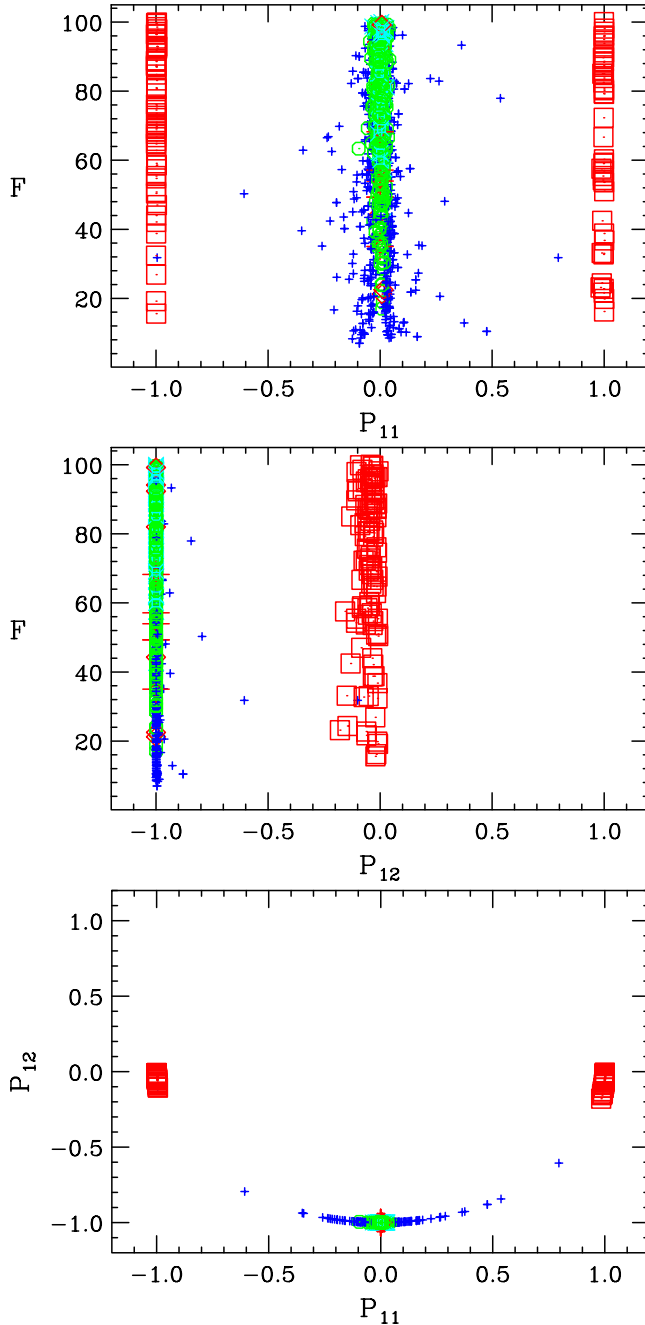


FIG. 11 (color online). For fixed $M_{1,2,3}(m_Z) = 100, 200, 300$ GeV and $\tan\beta = 10$ we plot: F vs P_{11} (top) and F vs P_{12} (middle). The bottom plot shows P_{12} vs P_{11} . Notation and conventions as in Fig. 6.

correspond to $-\sqrt{-m^2}$ with $m^2 < 0$. Low fine-tuning is often associated with one or more of the GUT-scale soft Higgs masses-squared being small. In particular, small $|m_{H_u}(M_U)|$ is needed for small F . Indeed, once $|M_{H_u}(M_U)|$ is above ~ 500 GeV, it is the parameter $p = m_{H_u}^2(M_U)$ that gives the maximum F_p and F becomes large. Note that the MSSM-like mixed-Higgs scenarios (large plain red squares) require $m_{H_u}(M_U) \sim 500$ GeV,

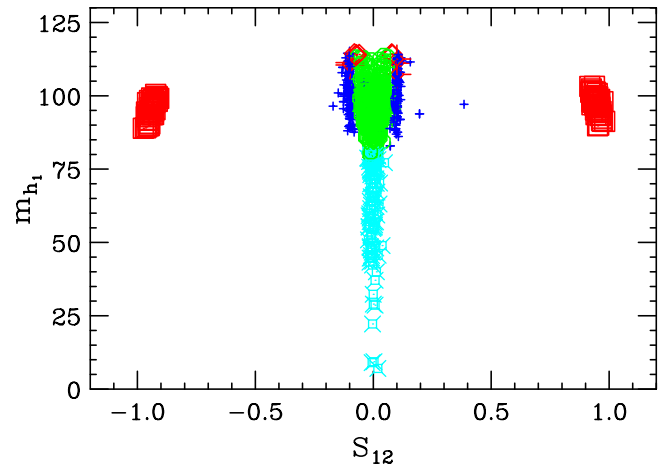


FIG. 12 (color online). For fixed $M_{1,2,3}(m_Z) = 100, 200, 300$ GeV and $\tan\beta = 10$ we plot: m_{h_1} vs S_{12} . Notation and conventions as in Fig. 6.

$m_{H_d}(M_U) \sim 0$, and modestly negative $m_S(M_U)$. The scenarios with large singlet mixing (green circles and cyan starred-squares) and fairly low F tend to have substantial $m_{H_u}(M_U)$ and $m_{H_d}(M_U)$, but relatively small $m_S(M_U)$. The low- F blue + scenarios with a light SM-like h_1 are more spread out in all these parameters, but are also easily obtained if all the GUT-scale soft Higgs masses-squared are relatively small.

It is also useful to examine F vs A_t and $A_t(M_U)$ as shown in Fig. 15. As noted in our earlier paper, the lowest F (blue) + points require quite small $A_t(M_U)$. (Of course, by “small,” we do not mean zero. Typically, all these parameters have magnitudes given by a scale of order 100–

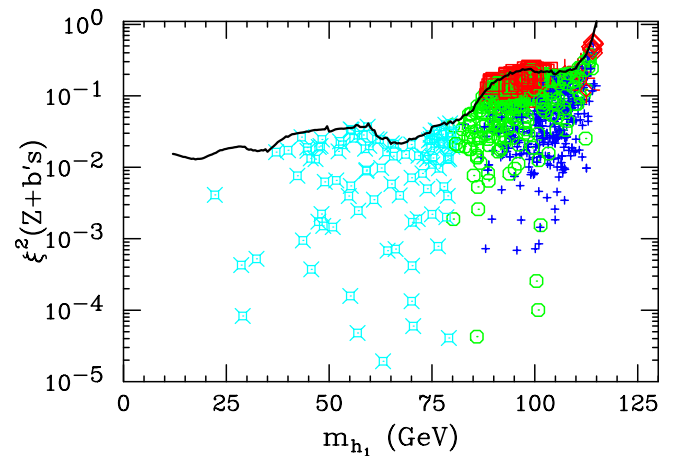


FIG. 13 (color online). For fixed $M_{1,2,3}(m_Z) = 100, 200, 300$ GeV and $\tan\beta = 10$ we plot $\xi^2(Z + b's)(h_1)$ vs m_{h_1} for the points from our scan. Also shown by the solid line is the approximate LEP experimental limit. Note the dip in this limit from about 60 GeV to about 80 GeV that cuts away scan points that would have survived with a slightly less severe limit. Notation and conventions as in Fig. 6.

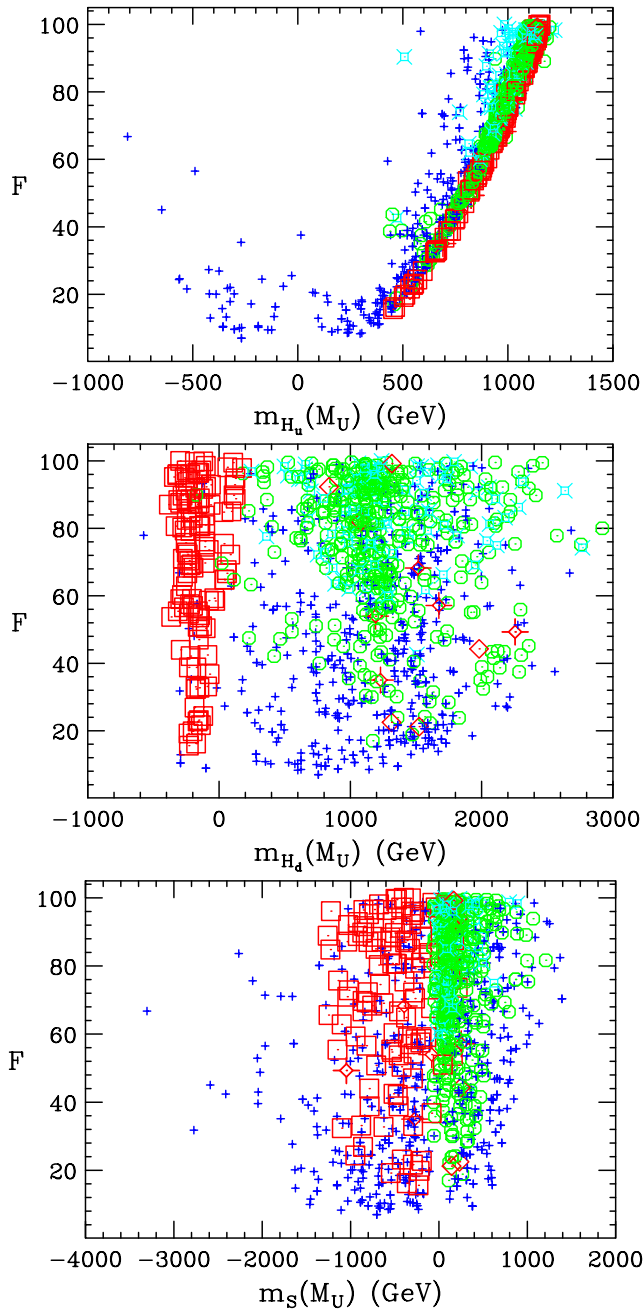


FIG. 14 (color online). For fixed $M_{1,2,3}(m_Z) = 100, 200, 300$ GeV and $\tan\beta = 10$ we plot F as a function of $m_{H_u}(M_U)$, $m_{H_d}(M_U)$, and $m_S(M_U)$, where negative m values are obtained as $-\sqrt{-m^2}$. Notation and conventions as in Fig. 6.

200 GeV, i.e. of order m_Z itself.) The lowest F values for the mixed-Higgs scenarios are achieved (as in the MSSM) for negative $A_t(m_Z) \lesssim -400$ GeV.

It is also amusing to examine F as a function of $m_Q(M_U)$, $m_U(M_U)$ and $m_D(M_U)$ for the third generation. The plots appear in Fig. 16. We observe that the smallest F (blue) + points require $m_Q(M_U)$, $m_U(M_U)$ and $m_D(M_U)$ values of order a few hundred GeV, while larger values are typically required for the various mixed-Higgs scenarios.

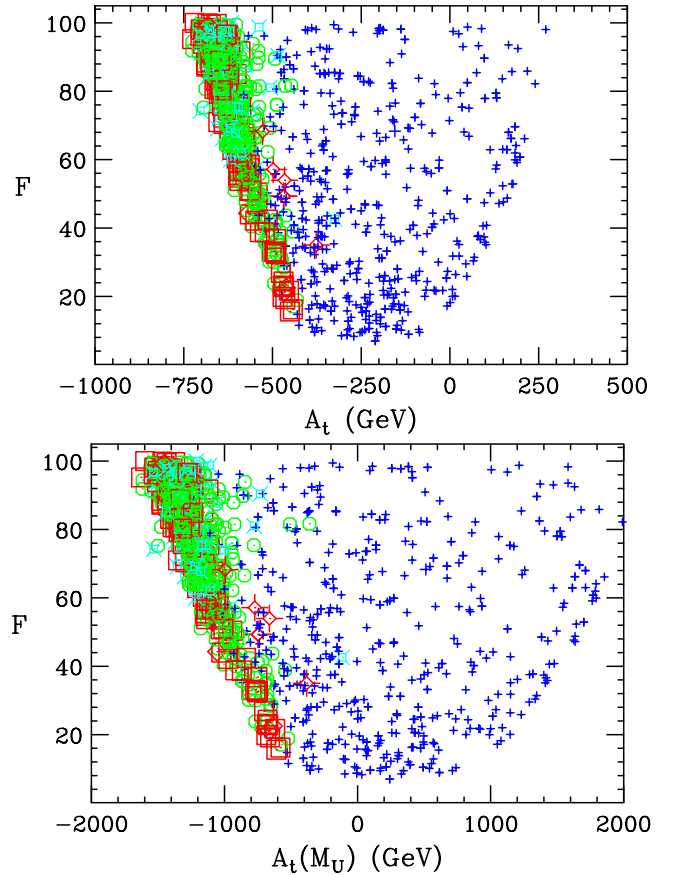


FIG. 15 (color online). For fixed $M_{1,2,3}(m_Z) = 100, 200, 300$ GeV and $\tan\beta = 10$ we plot F as a function of A_t (at scale m_Z) and of $A_t(M_U)$. Notation and conventions as in Fig. 6.

In Fig. 17, we show F as a function of $A_\lambda(M_U)$ and $A_\kappa(M_U)$. There is considerable spread. One noteworthy feature is that very small F values can be achieved for the (blue) +’s for $A_\lambda(M_U)$ and $A_\kappa(M_U)$ near zero. The other noteworthy feature is that the MSSM-like mixed-Higgs scenarios typically arise for substantial $A_\kappa(M_U)$.

Looking at Figs. 14–17 in an overall sense, we see that SUSY breaking Higgs, squark and mixing parameters should be chosen at the GUT scale according to at least an approximate, meaning $M_{\text{SUSY}} \lesssim \text{few} \times 100$ GeV, “no-scale” model of SUSY breaking in order to get the (blue) + points that minimize fine-tuning, whereas this is not true for the mixed-Higgs scenarios.

Next, in Fig. 18, we show F as a function of λ and κ . Note how the (blue) +’s with the very lowest F values populate a fairly distinct region from the mixed-Higgs scenario points. In particular, the singlet mixed-Higgs scenarios (green circles and cyan starred-squares) populate a region with $|\kappa| < 0.1$, whereas the (blue) +’s typically have $|\kappa| > 0.1$.

Finally, in Fig. 19, we give F as function of μ_{eff} . Obviously, small fine-tuning, whether in the mixed-Higgs scenarios or in the nontuned $m_{a_1} < 2m_b$ scenarios, requires μ_{eff} between the lower bound of about 120 GeV allowed by

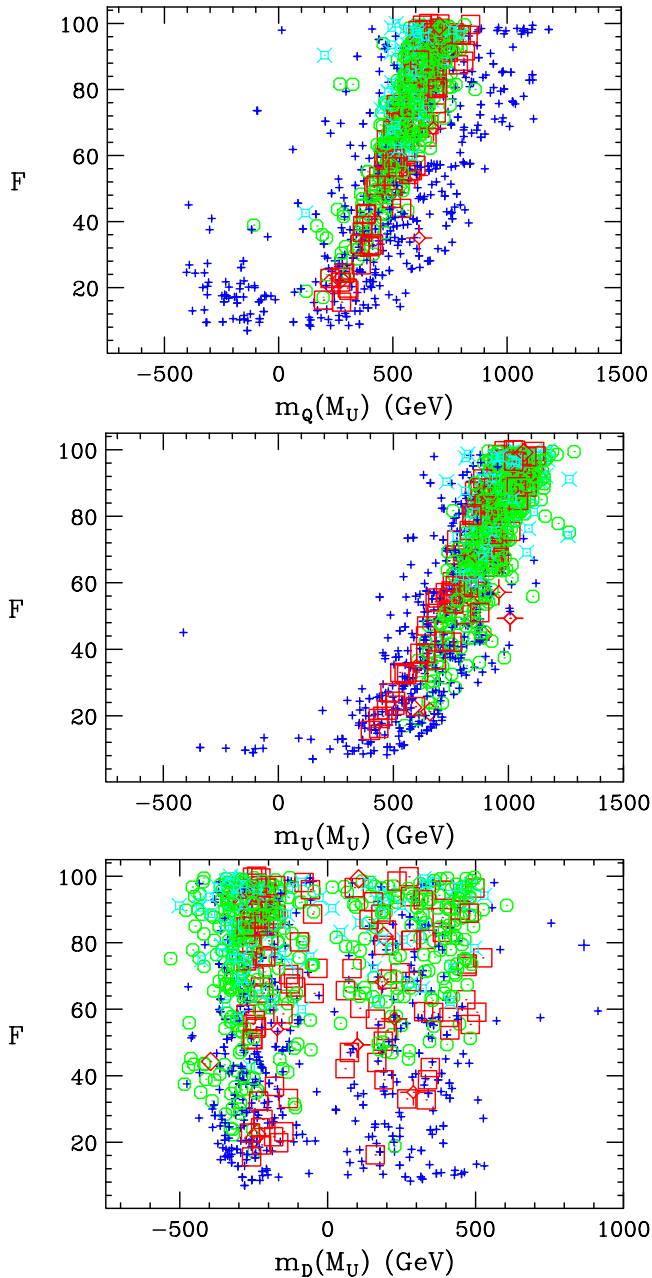


FIG. 16 (color online). For fixed $M_{1,2,3}(m_Z) = 100, 200, 300$ GeV and $\tan\beta = 10$ we plot F as a function of $m_Q(M_U)$, $m_U(M_U)$, and $m_D(M_U)$. For all three m 's, if $m^2 > 0$ ($m^2 < 0$) then $m \equiv \sqrt{m^2}$ ($m \equiv -\sqrt{-m^2}$). Notation and conventions as in Fig. 6.

LEP limits on the chargino mass and roughly 250 GeV. This would imply that charginos will be copiously produced and probably easy to detect at the LHC and ILC, and probably reachable in Tevatron late-stage running.

IV. CONCLUSIONS

In this paper, we have explored the degree of fine-tuning associated with mixed-Higgs scenarios, both in the MSSM

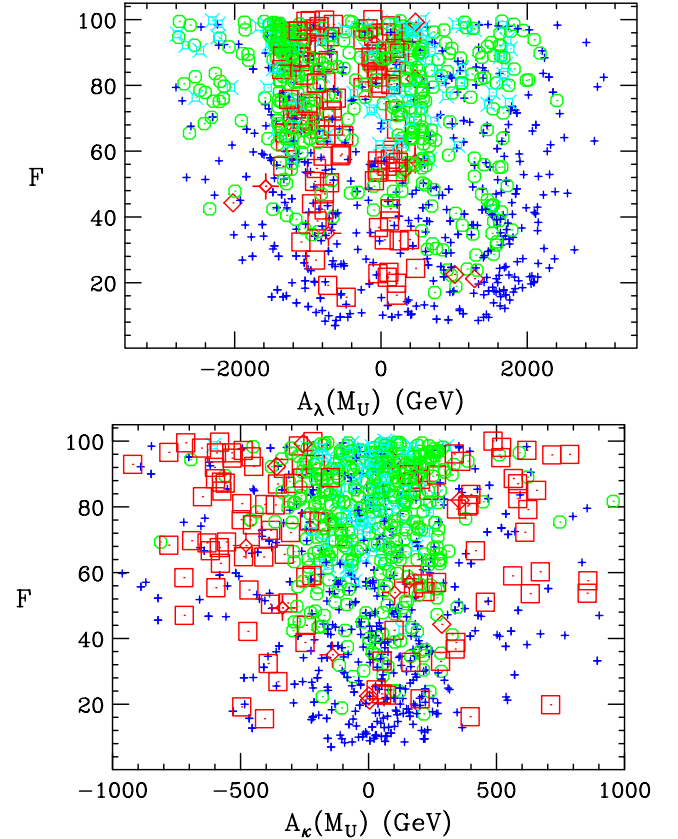


FIG. 17 (color online). For fixed $M_{1,2,3}(m_Z) = 100, 200, 300$ GeV and $\tan\beta = 10$ we plot F as a function of $A_\lambda(M_U)$ and $A_\kappa(M_U)$. Notation and conventions as in Fig. 6.

and the NMSSM. In the MSSM, we have seen that, relative to the usual decoupled scenarios with a lightest Higgs mass $m_h > 114$ GeV, mixed-Higgs scenarios allow a reduction in the fine-tuning, as measured by F of Eq. (2), of the GUT-scale model parameters in order to achieve correct EWSB. The smallest F achievable in the decoupled scenarios is $F \sim 30$, while mixed-Higgs scenarios can be found with $F \sim 16$. Thus, the mixed-Higgs MSSM scenarios give the smallest F values among those that are consistent with LEP limits.

In the NMSSM, there are many parameter choices for which the lightest Higgs has $m_{h_1} > 114$ GeV, but, as in the MSSM case, the minimum F values possible for such scenarios are large, $F \geq 20$. (This, however, is smaller than the minimum $F \sim 30$ achievable without Higgs mixing in the MSSM scenarios with $m_h > 114$ GeV.) In the NMSSM, further reduction in F is possible in two distinct cases. Scenarios corresponding to the first are those with substantial Higgs mixing for which $m_{h_1} < 114$ GeV is allowed by virtue of reduced ZZh_1 coupling. F values as small as ~ 16 (6.5% GUT-scale parameter tuning) are possible in this first class of models. Scenarios belonging to the second class are those where $m_{h_1} < 114$ GeV and the ZZh_1 coupling has full SM strength, but LEP constraints

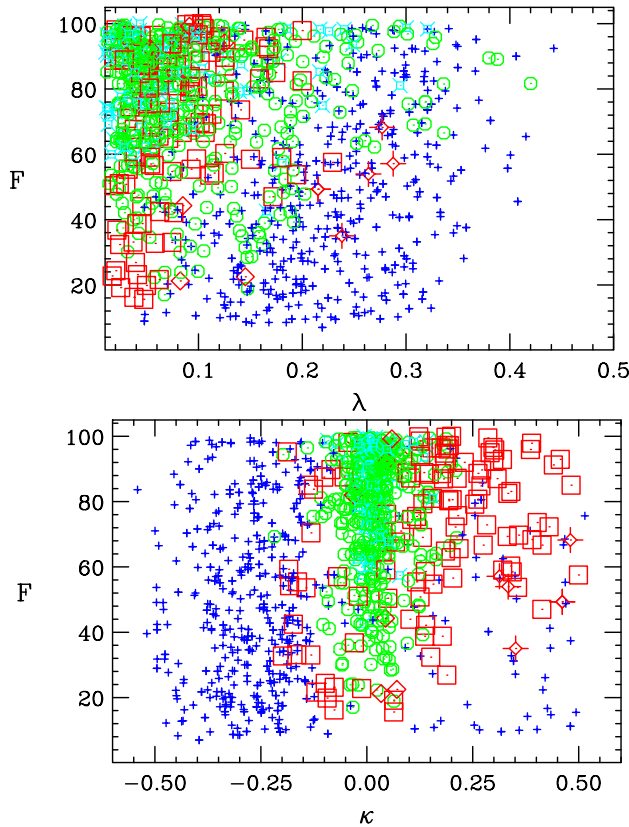


FIG. 18 (color online). For fixed $M_{1,2,3}(m_Z) = 100, 200, 300$ GeV and $\tan\beta = 10$ we plot F as a function of λ and κ . Notation and conventions as in Fig. 6.

are satisfied because the primary decay of the h_1 is $h_1 \rightarrow a_1 a_1 \rightarrow 4\tau$ or 4 jets. Values of F as small as ~ 6 (17% GUT-scale parameter tuning, which we regard as absence of fine-tuning) are possible in this case. This class of model is called the light- a_1 class. In a broad scan over parameter space, light- a_1 models emerge more or less immediately and automatically, whereas to find a significant number of

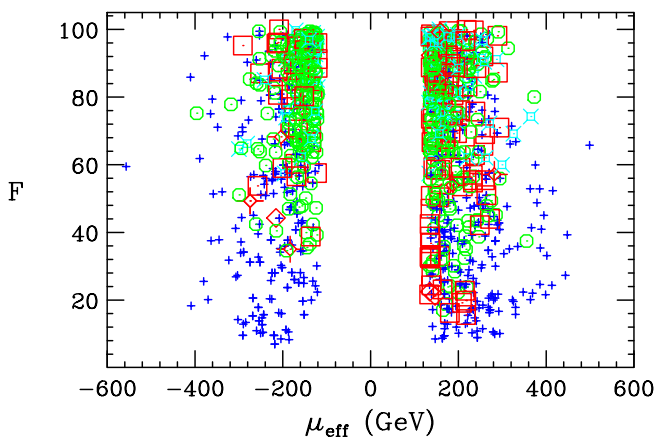


FIG. 19 (color online). For fixed $M_{1,2,3}(m_Z) = 100, 200, 300$ GeV and $\tan\beta = 10$ we plot F as a function of μ_{eff} . Notation and conventions as in Fig. 6.

mixed-Higgs scenario with reasonably low F requires highly focused scans.

The mixed-Higgs scenarios in the NMSSM can be divided into two classes: i) those in which the two doublet Higgs mix in close analogy with the mixed-Higgs MSSM scenarios; and ii) those in which there is substantial mixing of the doublet Higgses with the singlet Higgs. The former class arises when the singlet Higgs decouples from the doublet Higgses and there are many common features with the MSSM mixed-Higgs scenarios. In both the MSSM and class-(i) NMSSM mixed-Higgs scenarios, one finds the lowest F values for $m_{h_1} \sim m_{a_1} \sim 100$ GeV and $m_{h_2} \sim 120$ GeV. The corresponding soft-SUSY-breaking parameters are essentially the same as well; in particular, $A_t \sim -400$ GeV and $\bar{m}_{\tilde{t}} \sim 300$ GeV. In the class-(ii) NMSSM Higgs scenarios with large singlet mixing, a large range of m_{h_1} values is possible, but those with the smallest $F \sim 16$ values have $m_{h_1} \sim 100$ GeV and $m_{h_2} \sim 120$ GeV, as above, but a large range of possible m_{a_1} values; $A_t \sim -400$ and $\bar{m}_{\tilde{t}} \sim 300$ GeV are again needed.

The light- a_1 NMSSM scenarios are quite different in nature. Minimal F is achieved when the h_1 is very SM-like and has mass $m_{h_1} \sim 100$ GeV. For these scenarios, a large range of m_{h_2} is possible, beginning at $m_{h_2} \sim 150$ GeV and on up. The minimal F values are achieved for $A_t \sim -250$ GeV and somewhat smaller $\bar{m}_{\tilde{t}}$. GUT-scale Higgs and soft-SUSY-breaking parameters are relatively close to those expected for no-scale SUSY breaking. We have noted that the light- a_1 scenarios also provide a natural explanation of two crucial experimental observations: (1) the h_1 , having $C_V^2(h_1) \sim 1$ and $m_{h_1} \sim 100$ GeV, provides a natural explanation of the precision electroweak constraints; and (2) a value of $B(h_1 \rightarrow b\bar{b}) \sim 0.1$ is typical and yields a good description of the LEP excess in the $e^+e^- \rightarrow Z + b\bar{b}$ channel at $M_{b\bar{b}} \sim 98$ GeV.

The above can be contrasted with the mixed-Higgs scenarios. While these scenarios can also explain the excess of $Z + b\bar{b}$ events, the required values of $\xi^2(Z + b's) \sim 0.1$ and $m_{h_1} \sim 100$ GeV are only obtained if $F \geq 30$ —the lower $F \sim 16$ mixed-Higgs scenarios typically have $\xi^2(Z + b's) \sim C_V^2(h_1) \sim 0.2$ (see Figs. 8 and 13) and are thus only barely consistent with LEP limits. In comparison, light- a_1 scenarios with the lowest $F \sim 6$ values always have $m_{h_1} \sim 100$ GeV and a large fraction of these have $\xi^2(Z + b's) \sim 0.1$ (see Fig. 29 of Ref. [3]). In addition, a mixed-Higgs scenario with $m_{h_1} \sim 100$ GeV and $C_V^2(h_1) \sim 0.1$, to explain the LEP excess, always has an h_2 with $m_{h_2} > 114$ GeV and $C_V^2(h_2) \sim 0.9$, which combination does not yield nearly as good agreement with precision electroweak data as the light- a_1 scenarios that always have $m_{h_1} \sim 100$ GeV along with $C_V^2(h_1) \sim 1$.

All cases discussed above have differences that will be clear once experimental data for the Higgs sector become

available. One important test of the models will be consistency between the Higgs sector and the stop sector. In particular, large mixing in the stop sector plays a crucial role in the naturalness of EWSB in the MSSM. However, it is highly nontrivial to measure the mixing at colliders. Some methods to shed light on the mixing in the stop sector have been recently discussed in Refs. [24,25], but more work in this direction is certainly desirable.

While it is true that the above MSSM and NMSSM mixed-Higgs scenarios can have smaller fine-tuning (as we define it) than those yielding a light Higgs with mass above 114 GeV, these lower- F scenarios always require some additional restrictions (tuning) on other parameters, e.g. m_{H_d} and B_μ in the MSSM case and similar parameters in the NMSSM. This is to be contrasted with the fact that these same parameters are not particularly constrained in the cases where the lightest CP -even Higgs is SM-like. As a result of the parameter correlations required to obtain the mixed-Higgs scenarios with low F being significant, it might be very difficult to come up with models in which low- F mixed-Higgs scenarios are generic. In this respect, the light- a_1 NMSSM models may have an edge by virtue of

the fact that a light a_1 is quite naturally obtained as a result of a small breaking of the $U(1)_R$ symmetry limit of $A_\kappa(m_Z) = A_\lambda(m_Z) = 0$ via evolution from small A_κ and A_λ values at the GUT scale (see Refs. [26,27]). Typical values for $A_\kappa(M_U)$ and $A_\lambda(M_U)$ in the untuned $F \sim 6$ light- a_1 scenarios are shown in Fig. 17. In addition, such scenarios appear frequently for values of the GUT-scale Higgs masses-squared and a GUT-scale A_t value that are all close to zero (see Figs. 14 and 15 and further figures in Ref. [3]). Thus, the GUT-scale values for A_κ , A_λ , $m_{H_u}^2$, $m_{H_d}^2$, m_S^2 , and A_t are quite consistent with an approximate no-scale model of SUSY breaking in the case of light- a_1 scenarios with minimal fine-tuning.

ACKNOWLEDGMENTS

R. D. would like to thank N. Maekawa for helpful discussions. This work was supported by the U.S. Department of Energy under grants DE-FG02-90ER40542 and DE-FG03-91ER40674. J. F. G. also receives support from the U.C. Davis HEFTI program. J. F. G. thanks the Aspen Center for Physics where part of this work was performed.

-
- [1] R. Dermisek and J. F. Gunion, Phys. Rev. Lett. **95**, 041801 (2005).
- [2] R. Dermisek and J. F. Gunion, Phys. Rev. D **73**, 111701 (2006).
- [3] R. Dermisek and J. F. Gunion, Phys. Rev. D **76**, 095006 (2007).
- [4] J. R. Ellis, J. F. Gunion, H. E. Haber, L. Roszkowski, and F. Zwirner, Phys. Rev. D **39**, 844 (1989).
- [5] J. F. Gunion, H. E. Haber, and T. Moroi, arXiv:hep-ph/9610337.
- [6] U. Ellwanger, J. F. Gunion, and C. Hugonie, arXiv:hep-ph/0111179; U. Ellwanger, J. F. Gunion, C. Hugonie, and S. Moretti, arXiv:hep-ph/0305109; arXiv:hep-ph/0401228.
- [7] U. Ellwanger, J. F. Gunion, and C. Hugonie, J. High Energy Phys. **07** (2005) 041.
- [8] R. Barate *et al.* (LEP Working Group for Higgs boson searches), Phys. Lett. B **565**, 61 (2003).
- [9] LEP Working Group for Higgs Boson Searches, LHWG Report No. 2005-01.
- [10] A. Sopczak, Int. J. Mod. Phys. A **16S1B**, 816 (2001); Yad. Fiz. **65**, 2179 (2002) [Phys. At. Nucl. **65**, 2116 (2002)]; Nucl. Phys. B, Proc. Suppl. **109**, 271 (2002).
- [11] M. Carena, J. R. Ellis, A. Pilaftsis, and C. E. M. Wagner, Phys. Lett. B **495**, 155 (2000).
- [12] G. L. Kane, T. T. Wang, B. D. Nelson, and L. T. Wang, Phys. Rev. D **71**, 035006 (2005).
- [13] M. Drees, Phys. Rev. D **71**, 115006 (2005).
- [14] A. Belyaev, Q. H. Cao, D. Nomura, K. Tobe, and C. P. Yuan, arXiv:hep-ph/0609079.
- [15] S. G. Kim, N. Maekawa, A. Matsuzaki, K. Sakurai, A. I. Sanda, and T. Yoshikawa, Phys. Rev. D **74**, 115016 (2006).
- [16] R. Essig, Phys. Rev. D **75**, 095005 (2007).
- [17] M. Bastero-Gil, C. Hugonie, S. F. King, D. P. Roy, and S. Vempati, Phys. Lett. B **489**, 359 (2000).
- [18] D. J. Miller and S. Moretti, arXiv:hep-ph/0403137.
- [19] V. Barger, P. Langacker, H. S. Lee, and G. Shaughnessy, Phys. Rev. D **73**, 115010 (2006).
- [20] V. Barger, P. Langacker, and G. Shaughnessy, Phys. Rev. D **75**, 055013 (2007).
- [21] R. Dermisek and H. D. Kim, Phys. Rev. Lett. **96**, 211803 (2006).
- [22] H. P. Nilles, M. Srednicki, and D. Wyler, Phys. Lett. **120B**, 346 (1983); J. M. Frere, D. R. T. Jones, and S. Raby, Nucl. Phys. **B222**, 11 (1983); J. P. Derendinger and C. A. Savoy, Nucl. Phys. **B237**, 307 (1984); M. Drees, Int. J. Mod. Phys. A **4**, 3635 (1989); U. Ellwanger, M. Rausch de Traubenberg, and C. A. Savoy, Phys. Lett. B **315**, 331 (1993); Nucl. Phys. **B492**, 21 (1997); S. F. King and P. L. White, Phys. Rev. D **52**, 4183 (1995); F. Franke and H. Fraas, Int. J. Mod. Phys. A **12**, 479 (1997).
- [23] U. Ellwanger, J. F. Gunion, and C. Hugonie, J. High Energy Phys. **02** (2005) 066.
- [24] R. Dermisek and I. Low, arXiv:hep-ph/0701235.
- [25] M. Perelstein and C. Spethmann, J. High Energy Phys. **04** (2007) 070.
- [26] B. A. Dobrescu, G. Landsberg, and K. T. Matchev, Phys. Rev. D **63**, 075003 (2001); B. A. Dobrescu and K. T. Matchev, J. High Energy Phys. **09** (2000) 031.
- [27] R. Dermisek and J. F. Gunion, Phys. Rev. D **75**, 075019 (2007).